Clays and Clay Minerals, Vol. 54, No. 3, 295–313, 2006.

MINERALOGY AND GEOCHEMISTRY OF THE HOST-ROCK ALTERATIONS ASSOCIATED WITH THE SHEA CREEK UNCONFORMITY-TYPE URANIUM DEPOSITS (ATHABASCA BASIN, SASKATCHEWAN, CANADA). PART 2. REGIONAL-SCALE SPATIAL DISTRIBUTION OF THE ATHABASCA GROUP SANDSTONE MATRIX MINERALS

PHILIPPE KISTER[1,*], EMMANUEL LAVERRET[2], DAVID QUIRT[3], MICHEL CUNEY[1], PATRICIA PATRIER MAS[2], DANIEL BEAUFORT[2] AND PATRICE BRUNETON[4]

[1] UMR CNRS 7566 G2R-CREGU, UHP, BP 239, 54506 Vandœuvre-lès-Nancy Cedex, France
[2] HydrASA, UMR CNRS 6532, Université de Poitiers, 40 av. du Recteur Pineau, 86022 Poitiers Cedex, France
[3] Saskatchewan Research Council, 15 Innovation Blvd., Saskatoon, Saskatchewan, S7N 2X8, Canada
[4] COGEMA, Business Unit Mines, 2, rue Paul Dautier, BP 4, 78141 Velizy Cedex, France

Abstract—The spatial distribution of the dominant matrix minerals present in the middle-Proterozoic Athabasca Group sandstone (kaolin, illite, sudoite, dravite, hematite) was studied at a regional scale in the Shea Creek region (Saskatchewan, Canada), in which two epigenetic unconformity-type uranium deposits have been discovered. 3D models of matrix mineral distribution were derived from normative mineral calculations and 3D interpolation using whole-rock geochemical analyses of sandstone samples collected from both mineralized and barren areas. The calculations were constrained by information obtained from petrographic and crystal-chemical clay mineralogical studies on representative samples. The 3D mineral distribution models were compared to the lithostratigraphy and structural features of the Athabasca Group sandstone to ascertain the source and mobility of the main elements involved in the sandstone host-rock alteration processes related to the U mineralization. The distribution of Al is conformable with the lithostratigraphy throughout the studied area, regardless of proximity to basement-rooted structures and U ore bodies. The distribution of illite displays similar features, but the intensity of the illitization of kaolin decreases with increasing distance from the structures and U ore bodies. Hematite bleaching and neoformation of sudoite and dravite were restricted to the vicinity of the fault zones above the U ore bodies. The spatial configurations of the mineral anomalies show that syn-ore fluids flowed from the basement towards the sandstone cover *via* the fault zones, as described in current metallogenic models. Although Al remained immobile (mass transfer), the anomalous K, B and Mg present in the host-rock alteration haloes were probably imported from the basement rocks (mass transport). Unlike B and Mg, K migrated laterally at least several kilometers from the basement-rooted faults. The mineral distribution models were used to quantify the volume of altered sandstone (10^{-2}–10^{-1} km^3) and the amounts of K, Mg and B which were imported to the alteration haloes above the Shea Creek U ore bodies: 186,000 t of K, 66,000 t of Mg, and 11,000 t of B above the Anne ore body, and 24,000 t of K, 185,000 t of Mg, and a similar 11,000 t of B above the Colette ore body.

Key Words—3D Modeling, Athabasca Basin, Clay Minerals, Dravite, Host-rock Alteration, Illite, Kaolin, Normative Mineralogy, Unconformity-type Uranium Deposits, Sudoite.

INTRODUCTION

Clay minerals are sensitive indicators of the diagenetic history of sedimentary basins (Hurst and Irwin, 1982; Hoeve and Quirt, 1984; Lanson *et al*., 2002; Hutcheon, 2000; Berger *et al*., 1997, 1999; Hiatt and Kyser; 2000; Kyser and Hiatt, 2003, among others) and of host-rock alteration associated with sediment-hosted epigenetic ore deposits (Hoeve and Quirt, 1984; Skinner, 1997; Garven and Raffensperger, 1997; Reed, 1997; Kyser and Hiatt, 2003, among others). These minerals provide records of the different fluid-flow events that occurred in sedimentary basins, as their occurrence results from changes of the fluid physicochemical parameters (Hutcheon, 2000; Kyser and Hiatt, 2003). Consequently, determining the relative timing and spatial distribution of the clay mineral parageneses in sedimentary basins is of value for inferring the channels and directions in which the fluids flowed, especially those associated with ore deposition (Skinner, 1997; Kyser and Hiatt, 2003).

The world-class high-grade unconformity-type U deposits discovered in Saskatchewan (Canada) are examples of epigenetic deposits, the formation of which involved circulation of diagenetic brines in the middle-Proterozoic Athabasca sedimentary basin (Hoeve and Sibbald, 1978; Hoeve and Quirt, 1984; Kotzer and Kyser, 1995). The U ore is located close to the unconformity separating the Athabasca Group sediments

* E-mail address of corresponding author:
pkister@cogema.fr
DOI: 10.1346/CCMN.2006.0540302

and the underlying Archean–Paleoproterozoic crystalline basement rocks. The ore zones are spatially controlled by faults cross-cutting this unconformity. Redox-related U deposition occurred at sites of basement-sandstone fluid interaction along these structures. Uranium deposition was associated with the formation of clay-rich host-rock alteration haloes which envelop the main ore-controlling structures from a few tens of meters to several hundred meters around the U ore (Hoeve and Sibbald, 1978; Hoeve and Quirt, 1984; Pacquet and Weber, 1993; Percival *et al*., 1993; McGill *et al*., 1993; Kotzer and Kyser, 1995; Thomas *et al*. 2000; Lorilleux *et al*., 2002, 2003). These alteration haloes result from the interaction of the ore-forming fluids with the host-rocks and they overprinted the original sandstone and basement mineral parageneses. In this way, the host-rock alteration minerals record ancient mineralizing fluid-flow pathways and therefore constitute a major exploration guide to the location of U mineralization.

In this study we attempt to quantitatively determine the spatial distribution of the dominant matrix minerals in the Athabasca Group sandstone at a regional scale (~25 km) in the Shea Creek region, in which two unconformity-type U deposits (Anne and Colette zones) have been discovered (Rippert *et al*., 2000). The mineral compositions of the sandstone matrix were calculated using a normative procedure and whole-rock inductively coupled plasma-optical emission spectroscopy (ICP-OES) analyses of the Al, K, Fe, Mg and B contents of the sandstone. These calculations were constrained by information obtained from detailed petrographic and crystal-chemical clay mineralogical studies performed on representative samples (Laverret *et al*., 2006, this issue). The 3600 samples analyzed, collected from both mineralized and barren areas, were sufficient to allow 3D models of normative mineral distribution to be constructed at a regional scale. The spatial distribution of the matrix minerals was compared to the lithostratigraphy and structural features of the Athabasca Group sandstone to ascertain the relative mobility of the major elements involved in the host-rock alteration processes. The study shows that the formation of the host-rock alteration haloes above the U ore bodies required the transport of K, Mg and B from the basement, whereas Al remained relatively immobile. The 3D models were used to estimate the amount of K, B and Mg imported to the alteration haloes.

GEOLOGICAL SETTING

The geological setting and sandstone petrography of the Shea Creek region are described in detail by Laverret *et al*. (2006, this issue). A brief summary is given here.

The Athabasca Basin, (Saskatchewan, Canada) is filled by several dominantly orthoquartzitic clastic sequences, comprising variably hematitic, medium- to coarse-grained, fluviatile, quartz-rich sandstone, conglomerate, and minor siltstone, and lesser marine to lacustrine clastic sediments belonging to the Athabasca Group (Hoeve and Quirt, 1984; Ramaekers, 1990; Quirt, 2001; Ramaekers *et al*., 2001; Collier, 2002).

The Shea Creek U deposits (Anne and Colette zones) are located in the western part of the Athabasca Basin (Saskatchewan, Canada), 15 km south of the Carswell structure and ~300 km west of the majority of the U deposits (see Figure 1 in Laverret *et al*., 2006, this issue). The basement complex is composed of acidic to intermediate highly potassic igneous rocks, high-grade metamorphic sediments (up to granulite facies), and minor restites (Pagel and Svab, 1985; Card, 2002; Brouand and Cuney, 2002).

The overlying Athabasca-Group sediments, ~750 m thick in the study area, comprises five formations: Manitou Falls, Lazenby Lake, Wolverine Point, Locker Lake and Otherside (Laverret *et al*., 2006, this issue). The detrital mineralogy is similar to that described for the eastern part of the basin (Hoeve and Quirt, 1984; Armstrong and Ramaekers, 1985; Ramaekers, 1990; Kotzer and Kyser, 1995; Quirt, 2001), comprising dominant quartz, rare biotite, scarce white mica, and trace amounts of accessory minerals including zircon, Fe-Ti oxides, and Fe-tourmaline. No preserved feldspar mineral grains have been observed in the Athabasca Group. Some authors suggest that some clay mineral intraclasts may correspond to alteration products of former feldspar minerals (Hoeve and Quirt, 1984; Ramaekers, 1990; Quirt, 2001). However, diagenetic alteration of feldspar minerals in sandstone does not proceed by pseudomorphism and may rather lead to secondary porosity (Beaufort *et al.*, 1998).

The mineral paragenesis is consistent over the whole basin and consists of (1) early hematite, (2) secondary quartz overgrowths, (3) kaolin sub-group minerals (kaolin: kaolinite and dickite of the kaolinite–dickite series) as pore-filling cement and, to a lesser extent, as replacement of detrital micaceous minerals, and finally, (4) authigenic illite, occurring in the pore spaces, as replacement of kaolin and, occasionally, micaceous minerals (Hoeve and Quirt, 1984; Ramaekers, 1990; Laverret *et al*., 2006, this issue).

Two unconformity-type U deposits have been discovered in the Shea Creek region: the higher grade and tonnage Anne ore body, and the Colette ore body, located ~1.5 km NW of Anne along the same electromagnetic anomaly (Saskatoon Lake Conductor or SLC; Figure 1a,b). The SLC corresponds to an ~80 m wide, graphite-rich basement-rooted reverse fault zone, which cuts the sub-Athabasca unconformity and attenuates in the sandstone cover (Lorilleux *et al*., 2002). It is the main structural control of the U mineralization, which predominantly occurs at the unconformity in the basal Athabasca Group sandstone (MFc Formation) and, more locally, below the unconformity as high-grade veins in basement rocks.

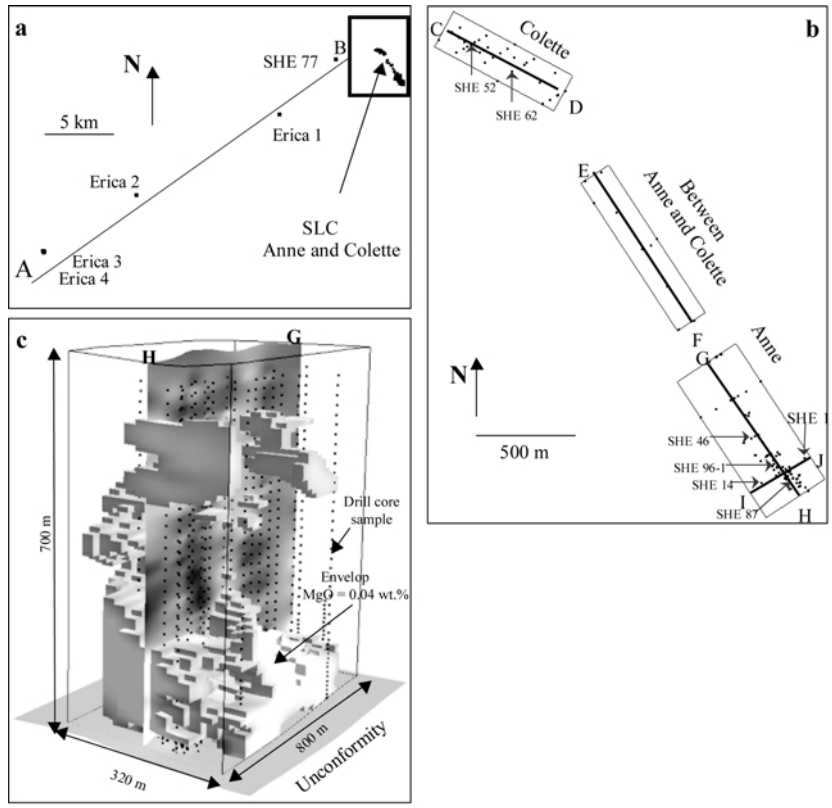

Figure 1. Locations of the exploration drill holes and the 3D modeling domains in the Shea Creek region. (a) Regional view: the drilling campaign essentially focused on the Saskatoon Lake Conductor (SLC). Section A–B is a 24 km cross-section perpendicular to the SLC in barren sandstone constrained by five drill holes. (b) Detailed view of drill hole locations along the SLC. The rectangles represent the boundaries of the domains considered for 3D modeling: Colette, Anne, and the region between Anne and Colette. Sections C–D to I–J are the representative vertical sections in the 3D models that are shown in Figures 5–7. (c) Example of 3D modelling in the Anne mineralized area: the figure shows the spatial distribution of the 0.04 wt.% MgO envelope.

In the Athabasca Basin, U deposition was associated with host-rock alteration, which overprinted the diagenetic assemblage of the sandstone and also replaced the original basement-rock minerals (Hoeve and Quirt, 1984; Kotzer and Kyser, 1995; Thomas *et al*., 2000). Typical ore-related alteration features include bleaching (removal of hematite), quartz dissolution (and consequent clay enrichment and local collapse of the host-rock), illitization, chloritization (Al-Mg di,trioctahedral chlorite (sudoite) and Mg-Fe tri,trioctahedral chlorite), neoformation of dravite and crandallite-group aluminum phosphate sulfate (APS) minerals. Petrographic studies of the Anne mineralized zone (Laverret *et al*., 2006, this issue) reveal that, in the sandstone cover, the syn-ore alteration halo is characterized by the occurrence of illite in replacement of kaolin. Sudoite is intergrown with illite in the innermost part of the alteration halo. Dravite occurs as acicular crystals associated both with illite and the illite-sudoite assemblage. In the basement, the ore-related alteration halo is of similar nature, although a tri,trioctahedral Mg-Fe chlorite has been identified in addition to sudoite. In the alteration haloes, both above and below the unconformity, illites are characterized by similar crystal textures, structures, and major element chemical compositions. Outside the alteration haloes, regional illites have different crystal textures and structures, but their major element chemical compositions are identical to those of illites in the alteration haloes (Laverret *et al*., 2006, this issue).

PROCEDURES

The matrix mineral composition of the Athabasca Group sandstone in the Shea Creek region was modeled through calculation of the normative mineralogy and then interpolated in 3D space. The normative calculations used the whole-rock geochemical data from the systematic sampling of the exploration drill cores by Cogema Resources Inc. The matrix mineral compositions obtained by normative calculations were compared with those obtained by X-ray diffraction (XRD) analyses performed on sandstone core samples. This procedure was not applied to basement rock samples because of their heterogeneous lithologies, fine-scale mineral compositional variations, and their complex structural relationships, which are only documented for small

intervals (<100 m) below the unconformity, a limitation imposed by the end of the drill holes. Conversely, the mineralogy of the Athabasca Group sandstone is relatively simple and is well suited to normative calculations, as it consists dominantly of quartz with only minor Al-bearing phases, including kaolinite, illite, sudoite and dravite (Quirt, 1995). In addition, the Athabasca Group comprises flat-lying lithological units, which can be easily represented in 3D space.

Whole-rock geochemical database

In all, 105 vertical diamond drill holes and 54 directional drill holes extending from some of the vertical drill holes have been completed in the Shea Creek region. They were mainly drilled along the SLC, in particular in the Anne and Colette mineralized areas (Figure 1). The vertical boreholes were drilled from the surface to depths of >800 m through the Athabasca Group sandstone, the underlying unconformity, and into the crystalline basement. The drilling pattern was a grid at an initial 100 m spacing, with a 40 m lateral spacing where mineralization was intersected. Because of the lesser mineralization encountered in the Colette area, the drill hole density is less there than in the Anne area (Figure 1b).

In addition, five other vertical boreholes (She 77; Erica 1, 2, 3 and 4, referred to as the 'distal drill holes') were drilled away from the Shea Creek mineralized area at ~5 km intervals along a section perpendicular to the SLC (Figure 1a). Only drill hole Erica 1 did not intersect any basement-rooted faults or electromagnetic conductors and only in drill hole Erica 3 were traces of U detected near the unconformity.

More than 3600 core samples were taken from these drill holes for whole-rock geochemical analyses. In unmineralized areas, samples were systematically collected every 10 m, whereas the high-grade ore zones were continuously sampled using split core.

The samples were prepared and analyzed for major and trace elements (Al, Mg, K, Pb, U, B, Fe, Mo, Zn, Co, V, Cu, Ni, Bi, As) at the Saskatchewan Research Council Geoanalytical Laboratory. The elements of interest to this study are Al, Mg, K, Fe and B. Sample preparation consisted of steel-jaw crushing followed by grinding in a steel puck and ring grinder. Two sample digestions were performed on portions of the whole-rock (bulk sample) pulp and all samples were analyzed using multi-element ICP-OES techniques. The first digestion was an Aqua Regia (HCl-HNO_3) partial digestion on a 500 mg portion of the sample and the second digestion was a total digestion using a tri-acid attack (HF-HNO_3-$HClO_4$) on 125 mg of sample. Boron was determined following sample fusion with Na_2O_2 and acid dissolution. The detection limits and precision are: 0.01±0.02 wt.% for Al_2O_3 and Fe_2O_3, and 0.01±0.02 wt.% to 0.001±0.003 wt.% for MgO and K_2O, depending on the year of analysis, and 1±1 ppm for B, respectively.

Normative mineral calculations

The normative mineral contents of Athabasca Group sandstone matrix were calculated using whole-rock data for Al_2O_3, K_2O, MgO, total iron as Fe_2O_3, and B. SiO_2 was not analyzed. The mineral chemical compositions used in the calculation of the normative minerals were based on data from previous mineralogical studies (see below). B, K, Mg, Al and Fe were allocated to the normative minerals in a specific sequence (Quirt, 1995): (1) first, B and K are quantitatively allocated to dravite and illite, respectively, as these elements each reside in only one mineral, along with some Al, Fe and/or Mg; (2) then, any remaining Mg is allocated to sudoite; (3) any remaining Al and Fe are allocated to kaolinite and hematite, respectively. The normative mineral absolute contents are expressed in wt.%.

The chemical compositions of illite and sudoite were obtained from mineralogical studies of sandstone from the Shea Creek area (Laverret, 2002; Laverret *et al.*, 2006, this issue). Electron microprobe analyses of illite provide a very homogeneous chemical composition of $(K_{0.805}Na_{0.015}Ca_{0.015})(Mg_{0.15}Fe_{0.05}Al_{1.8})(Al_{0.7}Si_{3.3})O_{10}(OH)_2$ both in unaltered and altered areas. The variations in the main cation proportions (Si, Al, K and Mg) are <2%, which is in the same order as the analytical uncertainties.

Pure chemical compositions of sudoite were rarely obtained by electron microprobe analysis because sudoite is usually very finely intergrown with illite in the Shea Creek region (Laverret, 2002). However, the few analyses of pure sudoite from this region give homogeneous compositions close to the composition of one group of sudoite determined by Billault *et al.* (2002) in sandstone samples located west of the Cigar Lake deposit: $(Mg_{1.65}Fe^{3+}_{0.03}Fe^{2+}_{0.02}Al_{3.11})(Al_{0.77}Si_{3.23})O_{10}(OH)_8$. As the variations in the cation contents are of the same order as the analytical uncertainties (Laverret, 2002), sudoites in the Shea Creek district are assumed to have a similar composition.

The chemical composition of dravite has not been determined for samples in the Shea Creek area. However, analyses of dravite occurring in the eastern part of the Athabasca Basin give a structural formula of $Na_{0.26}(Mg_{2.04}Fe_{0.09}Al_{1.05})Al_6(Si_6O_{18})(BO_3)_3(OH,F)_4$ (Quirt *et al.*, 1991). The ideal structural formula of kaolinite ($Al_2Si_2O_5(OH)_4$) has been used for all kaolin sub-group minerals and the term 'normative kaolinite' is used in this study to designate any kaolin sub-group mineral with no specification of the polymorph.

XRD analyses

X-ray diffraction analyses of the <5 μm size fraction were conducted by the Saskatchewan Research Council (SRC) on 1100 samples taken from the 3600 systematic exploration samples, *i.e.* at every 60 m in the upper sandstone formations, and at closer intervals near the unconformity, from ~60 exploration drill holes both in the

Anne and Colette areas. The <5 μm fraction was obtained from the sample pulps, as previously prepared for geochemical analysis at the SRC, by centrifuging techniques similar to those outlined by Jambor and Dilabio (1978). The extracted clay mineral slurry was transferred to glass slides by the slurry-smear technique which provides an oriented specimen suitable for quantitative analysis of the relative proportion of sudoite, illite and kaolin, but with relatively poor distinction of the clay mineral polytypes and/or polymorphs.

The XRD analyses of the <2 μm size fraction were conducted on specific samples selected from six representative drill holes (Erica 1, Erica 3, She 77, She 14, She 11, She 87: Figure 1; Laverret *et al.*, 2006, this issue). These analyses provided an accurate determination of the neoformed clay mineral polytypes and polymorphs as the freeze-thaw sample disaggregation procedure used avoided contamination from coarse-grained detrital material, such as mica, but the results were only semi-quantitative.

3D representation

The spatial distribution of the normative minerals (illite, dravite, sudoite, kaolinite and hematite) and Al_2O_3 contents have been modeled in 3D space using the GOCAD modeling software. The sample data are modeled as a set of points referenced by their geographical coordinates coupled with the Discrete Smooth Interpolation method (Mallet, 1992). The dimensions of the grid cells were $20 \times 30 \times 10$ m^3 in the sandstone where samples were collected every 10 m and $20 \times 30 \times 1$ m^3 close to the mineralized zones, which were continuously sampled. The 3D distribution models were constructed over a large volume, comprising (1) three sets along the SLC (Figure 1b) including the Anne mineralized area (820 m × 320 m × 700 m, Figure 1c), the Colette mineralized area (620 m × 180 m × 700 m), and the region between the Anne and Colette areas (800 m × 150 m × 700 m), and (2) a 24 km long distal section through unmineralized sandstone ('distal section'; Figure 1a).

Table 1. Estimation of the K, B and Mg surplus in the host-rock altered Anne and Colette areas relative to the background Erica 1 drill hole.

	K surplus		Mg surplus		B surplus	
	tonnage (a)	volume (b)	tonnage (a)	volume (b)	tonnage (a)	volume (b)
Anne						
Total	1.86×10^5	7.98×10^{-2}	6.61×10^4	3.03×10^{-2}	1.08×10^4	4.84×10^{-2}
Detail per lithogeochemical units						
WP+LL	4.85×10^4	4.32×10^{-2}	4.35×10^3	6.25×10^{-3}	4.54×10^3	2.42×10^{-2}
UpperLzL	5.28×10^4	1.57×10^{-2}	1.64×10^3	1.65×10^{-3}	6.21×10^2	2.51×10^{-3}
LowerLzL	2.44×10^4	7.97×10^{-3}	2.66×10^3	3.62×10^{-3}	8.79×10^2	6.04×10^{-3}
MFd	3.12×10^4	7.43×10^{-3}	5.54×10^3	6.00×10^{-3}	1.42×10^3	6.71×10^{-3}
UpperMFc	2.34×10^4	3.80×10^{-3}	5.05×10^3	6.29×10^{-3}	8.57×10^2	4.58×10^{-3}
LowerMFc	5.54×10^3	1.68×10^{-3}	4.68×10^4	6.45×10^{-3}	2.54×10^3	4.39×10^{-3}
Colette						
Total	2.42×10^4	8.71×10^{-3}	1.85×10^5	7.84×10^{-2}	1.15×10^4	7.72×10^{-2}
Detail per lithogeochemical units						
WP+LL	4.98×10^3	4.20×10^{-3}	3.61×10^4	3.80×10^{-2}	5.34×10^3	3.85×10^{-2}
UpperLzL	9.55×10^2	9.15×10^{-4}	4.02×10^4	1.02×10^{-2}	1.68×10^3	1.02×10^{-2}
LowerLzL	5.46×10^2	3.24×10^{-4}	4.72×10^4	1.07×10^{-2}	8.64×10^2	1.07×10^{-2}
MFd	1.50×10^1	3.37×10^{-5}	2.24×10^4	9.03×10^{-3}	9.36×10^2	8.88×10^{-3}
UpperMFc	1.43×10^4	2.23×10^{-3}	1.56×10^4	6.21×10^{-3}	1.70×10^3	6.21×10^{-3}
LowerMFc	3.39×10^3	1.01×10^{-3}	2.33×10^4	4.28×10^{-3}	9.43×10^2	2.80×10^{-3}

Threshold contents (c)			
	K_2O (wt.%)	MgO (wt.%)	B (ppm)
WP+LL	0.17	0.02	17
UpperLzL	0.14	0.01	11
LowerLzL	0.40	0.04	26
MFd	0.19	0.04	20
UpperMFc	0.58	0.05	30
LowerMFc	0.10	0.03	42

Notes: (a) unit: metric tonne (see text for procedure); (b) unit: km^3; (c) corresponds to the 75th percentile value of the background samples from drill hole Erica 1. As the element contents are (at least partly) controlled by the lithology, specific threshold values have been chosen for each lithological unit. Formation abbreviations: MF: Manitou Falls; LzL: Lazenby Lake; WP+LL: Wolverine Point + Locker Lake.

Mass-balance calculations

The surplus amounts of K, B and Mg (m_x) necessary to form the illite, sudoite and dravite anomalies above the Anne and Colette ore bodies (see below), were calculated by applying the following formula to the 3D grids of the GOCAD models:

$$m_x = \sum_{\text{cell}} (x_{\text{cell}} - x_0)\nu_{\text{cell}} \quad (1)$$

Here, the rock density ($\square$) used was 2.5 t/m^3 for all cells. ν_{cell} represents the cell volume and x_{cell} represents the K, B or Mg content of a cell. The sum ($\square_{\text{cell}}$) accounts only for the cells in which the K, B or Mg content exceeds a threshold content, x_0. The threshold K, B and Mg contents were obtained for each lithological unit using the data for samples from drill hole Erica 1. They correspond to the 75$^{\text{th}}$ percentile values (Table 1). Drill hole Erica 1 was chosen as the background reference because it is the least affected by host-rock alterations (Laverret *et al.*, 2006, this issue).

RESULTS

Normative mineral composition

Before proceeding with 3D interpolation, the calculated normative mineralogy was compared with the XRD analytical data to check the consistency between the two approaches and to estimate how closely the normative calculation procedure approximates the mineral composition of the Athabasca sandstone intergranular matrix.

The semi-quantitative XRD data for the <2 μm fraction (Laverret *et al.*, 2006, this issue) and the normative data for two representative drill holes (Erica 1: unaltered, and She 87: the most altered and

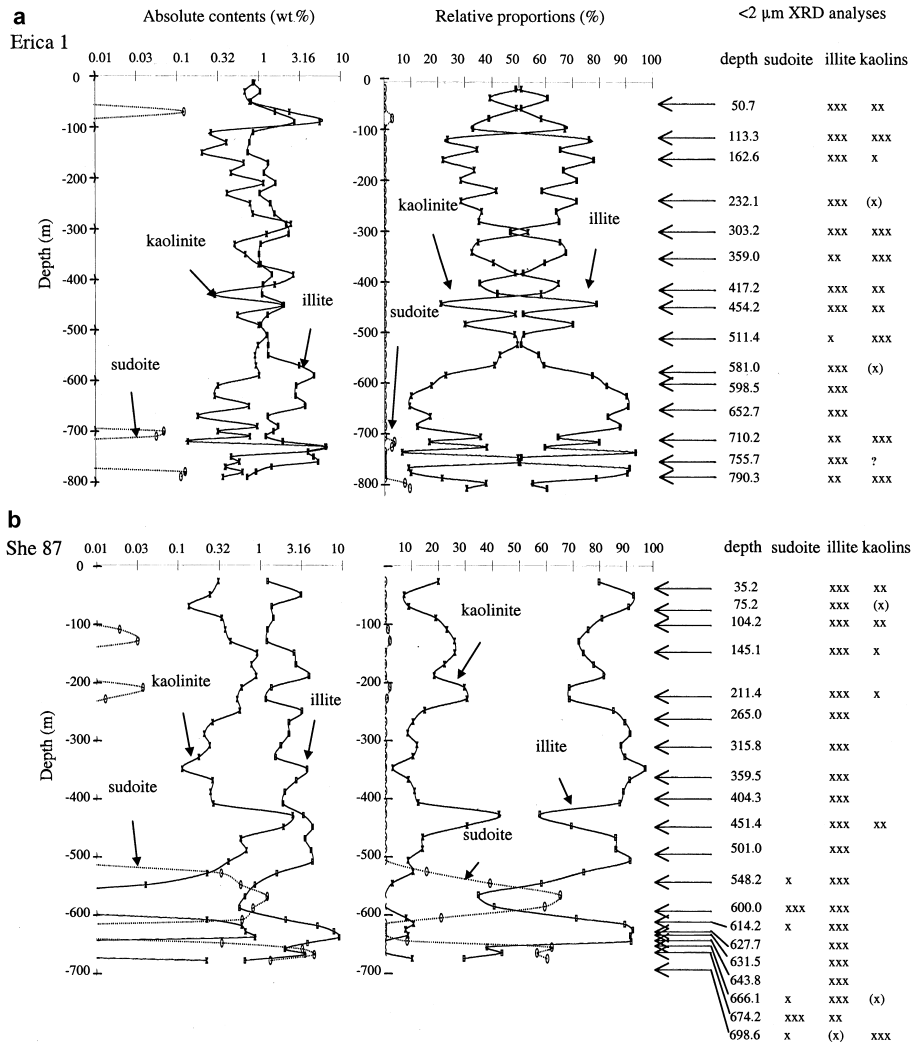

Figure 2. Comparison of the semi-quantitative XRD analyses of the <2 μm fraction (Laverret *et al.*, 2006, this issue) with the normative clay mineral composition (expressed as both absolute content and relative proportion). (a) Drill hole Erica 1 (the least altered); (b) drill hole She 87 (cross-cuts the Anne ore body). (X): small amount; XXX: large amount; ?: suspected. Drill holes Erica 1 and She 87 are indicated in Figure 1.

intersecting the Anne ore zone) are compared in Figure 2. The relative proportions of illite and kaolin obtained by XRD compares well, qualitatively, with the relative proportions of normative illite and kaolinite. A similar consistency is observed for sudoite (Figure 2), which was detected by XRD in only six samples from drill hole She 87 at depths of ~575 m and ~680 m, which correspond to the depths where the highest normative sudoite contents have been obtained (>0.2 wt.%).

The quantitative XRD analytical results for the <5 μm fraction are compared with the calculated normative mineralogy in Figure 3. Overall, there is good agreement between the relative proportions of illite, sudoite and kaolinite. Very similar patterns of clay mineral proportions are observed, both in the absence (Erica 1) or presence of sudoite (She 14, 46, 52, 62). However, compared to the XRD data, the norm calculation procedure appears to underestimate the proportion of illite (Erica 1, She 62) and to overestimate the proportion of kaolin (up to 25% error in She 52). These discrepancies result from the presence of mineral size fractionation, or the variation in clay mineral proportions in the different size fractions. The normative data are based on whole-rock analyses while the XRD data are obtained by analysis of the <5 μm size fraction. The relatively large blocky dickite crystals, which often exceed 10 μm in size, are not present in the size-fraction used for the XRD analyses (Quirt, 1995, 2001). This effect is accentuated by the fact that illitization of kaolin preferentially affects the smaller vermicular kaolinite crystals rather than the larger blocky dickite crystals (Hoeve and Quirt, 1984; Lanson *et al*., 2002; Beaufort *et al*., 1998).

Another cause for overestimation of the kaolin proportion by the normative calculation procedure is the presence of other Al-bearing minerals in the sandstone, such as APS minerals. As normative kaolinite represents the Al remaining following calculation of normative sudoite, illite and dravite, it also includes Al present in any other Al-bearing minerals. However, APS minerals are typically only present in trace amounts in the Athabasca Group, except locally in the highly fractured and altered zones around the U ore bodies (Wilson, 1984; Lorilleux *et al*., 2003). Consequently, the small amount of Al provided by these minerals is insignificant at the scale of the study area.

The proportion of normative sudoite shows good agreement with the XRD analyses for samples with small illite and kaolinite proportions (*e.g.* She 52 or She 62 from 525 to 625 m, Figure 3), but it appears to be overestimated with respect to the XRD values when illite and kaolin are present in significant amounts (*e.g.* She 62 from 300 to 450 m). This is a consequence of the underestimation of the absolute content of illite, as noted above, because the normative procedure calculates the amount of normative sudoite following subtraction of the Mg contained in normative illite. Another possible cause may be the variability of the sudoite crystal chemistry, but the few analyses of sudoite in the Shea Creek deposit indicate homogeneous compositions.

For dravite and hematite, no quantitative XRD data are available to check the consistency of the normative calculations. However, the amount of normative dravite should be reasonably estimated, as detrital Fe-tourmaline is present in negligible amounts relative to dravite. Conversely, the hematite content may be overestimated because normative hematite is allocated the Fe remaining following subtraction of the Fe contained in illite and sudoite, and other Fe-bearing minerals (pyrite, siderite) may be locally present (Hoeve and Quirt, 1984; Pacquet and Weber, 1993; Lorilleux *et al*., 2003). However, petrographic observations indicate that pyrite is only present in the ore zone and siderite is rarely present and in only trace amounts in the sandstone cover.

3D representation

The normative mineral contents were interpolated over a large volume comprising both distal and proximal zones to basement-rooted structures (Figure 1). The Al_2O_3 data were also interpolated because the Al content is proportional to the total aluminosilicate content (clay minerals + dravite). For example, a perspective view of one of these 3D representations is shown in Figure 1c. In the following, we are showing representative vertical sections across these 3D models (Figures 4, 6 and 7), comprising (1) a 24 km long section perpendicular to the SLC, termed the 'distal section' (A–B, Figure 1a), (2) three longitudinal sections along the SLC (Figure 1b), including the Colette ore zone (C–D), the Anne ore zone (G–H), and the region between Anne and Colette (E–F), and (3) a 320 m lateral section that crosses the Anne high-grade U ore body (I–J).

Al_2O_3

The 3D distribution models of the Al_2O_3 data highlight relatively Al-rich horizons that parallel the stratigraphy (Figure 4) in the upper half of the MFc and lower half of the LzL Formations, in contrast to the MFd Formation which has the smallest Al_2O_3 contents (Table 2). These features are observed over the entire modeled area, *i.e.* both above the SLC where the U ore bodies are located, and along the distal section perpendicular to the SLC (Figure 4). Within a given Formation, only slight variations in Al_2O_3 content are present between the different zones (Table 2). In the upper MFc, lower LzL and MFd Formations, the mean Al_2O_3 values only vary between 2.3 and 2.8 wt.%, 1.1 and 1.6 wt.%, and 0.5 and 1.0 wt.%, respectively.

In the immediate vicinity of the Anne and Colette U ore bodies, the Al_2O_3 contents vary widely within the lower MFc Formation from minima of 0.27 wt.% and 0.30 wt.% to maxima of 26.16 wt.% and 29.90 wt.%, respectively (Table 2). These variations in Al_2O_3 are

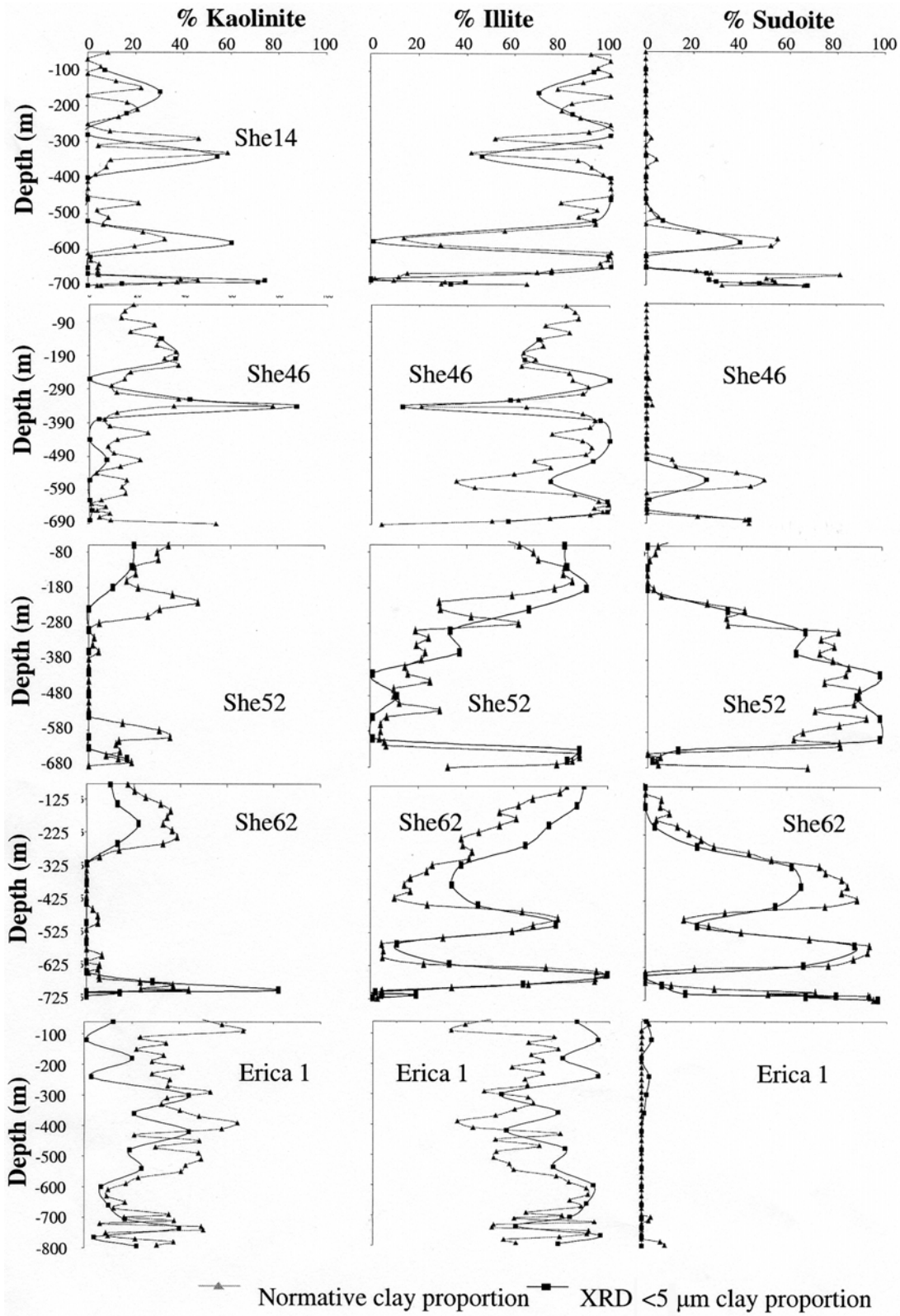

Figure 3. Comparison of the quantitative XRD analyses of the <5 μm fraction with the normative clay mineral composition. The results are shown for five representative drill holes: She 14 and 46 (Anne area), She 52 and 62 (Colette area), and Erica 1 drill hole. See Figure 1 for the locations of the drill holes.

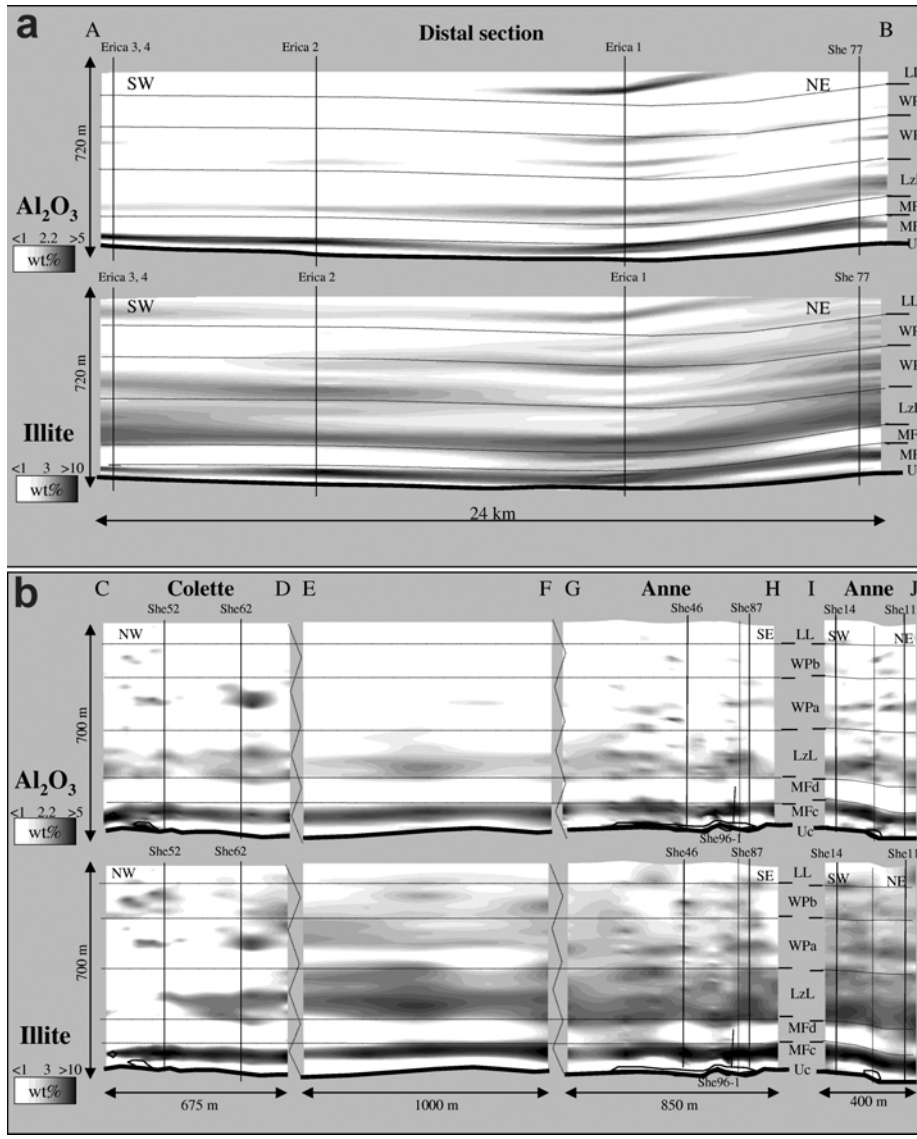

Figure 4. Al_2O_3 (upper) and illite (lower) spatial distributions. The figure shows a vertical section across the 3D models (see Figure 1c). (a) Distal section, A–B, perpendicular to the SLC and constrained by five drill holes. Only drill hole Erica 1 did not intersect any basement-rooted structure. (b) Sections across the mineralized areas of Anne and Colette along the SLC (longitudinal sections: C–D, E–F, G–H; lateral section: I–J). Only the most representative drill holes used in the text are shown (white vertical line). White indicates smaller contents; black, greater contents. Black outline: high-grade ore zone (U >500 ppm). Abbreviations: LL, WP, LzL, MF, Uc are Locker Lake, Wolverine Point, Lazenby Lake, Manitou Falls Formations, and unconformity, respectively.

large relative to those for the overlying units and are in contrast to the distal and Erica 1 drill holes, which have Al_2O_3 mean values consistently <1 wt.%.

Normative illite

The spatial distribution of the normative illite contents displays features similar to that of Al_2O_3 (Figure 4): the upper MFc and lower LzL Formations are illite-rich (3.9–5.5 wt.% and 1.6–3.3 wt.%, respectively, Table 2) and contrast with the MFd Formation, which has a small illite content (0.3–2.0 wt.%). This distribution pattern is observed over the entire Shea Creek region, except in the NW part of the Colette area, where sudoite is predominant (Figure 4).

The positive correlation between illite and alumina is also highlighted on a K *vs*. Al diagram (Figure 5). The K data reflect the normative illite contents, as all K is allocated to illite in the normative procedure. The K/Al ratio is used as an indicator of the intensity of illitization of kaolin, rather than the absolute amount of illite, because the absolute illite content varies proportionally with the initial amount of kaolin. This situation is not valid when significant amounts of sudoite are present (>0.4 wt.%) because sudoite also occurs as a replace-

Table 2. Summary of the normative mineral and Al_2O_3 contents (wt.%) in the Anne area, Colette area, distal drill holes (Erica 2, 3, 4, She 77), and drill hole Erica 1.

Unit	Minimum				Maximum				Mean				Standard deviation			
	Anne[a]	Colette[b]	Distal[c]	Erica 1[d]	Anne[a]	Colette[b]	Distal[c]	Erica 1[d]	Anne[a]	Colette[b]	Distal[c]	Erica 1[d]	Anne[a]	Colette[b]	Distal[c]	Erica 1[d]
Al_2O_3																
WP+LL	0.38	0.40	0.34	0.36	3.64	5.20	2.40	3.24	0.86	0.80	0.67	0.98	0.41	0.50	0.31	0.66
UpperLzL	0.60	0.60	0.51	0.53	2.34	2.30	1.18	1.52	1.05	0.90	0.75	0.83	0.30	0.30	0.17	0.34
LowerLzL	0.27	0.60	0.67	0.84	3.84	4.70	1.49	2.16	1.61	1.50	1.07	1.55	0.57	0.50	0.26	0.56
MFd	0.42	0.40	0.32	0.56	1.78	1.70	1.19	1.68	0.77	0.70	0.54	0.78	0.26	0.22	0.20	0.4
UpperMFc	0.66	0.50	0.37	0.79	6.81	9.90	4.98	5.01	2.82	2.50	2.30	3.05	1.03	1.50	1.64	1.59
LowerMFc	0.27	0.30	0.39	0.48	26.16	29.90	2.23	0.72	3.20	4.40	0.96	0.64	4.48	5.95	0.50	0.17
Kaolinite																
WP+LL	0.01	0.01	0.01	0.20	6.78	7.64	5.57	5.57	0.41	0.45	0.52	1.20	0.51	0.63	0.80	1.22
UpperLzL	0.01	0.01	0.08	0.29	1.84	2.08	1.90	1.91	0.37	0.02	0.41	0.92	0.33	0.18	0.42	0.56
LowerLzL	0.01	0.01	0.01	0.31	5.29	6.76	0.99	0.99	0.82	0.14	0.36	0.65	0.90	0.60	0.28	0.31
MFd	0.01	0.01	0.02	0.18	0.85	0.57	0.94	0.94	0.23	0.07	0.29	0.47	0.17	0.12	0.25	0.32
UpperMFc	0.01	0.01	0.14	0.13	2.30	10.39	6.42	6.42	0.41	0.52	0.90	2.85	0.36	1.03	1.28	2.56
LowerMFc	0.01	0.01	0.01	0.36	49.51	2.19	4.08	0.62	1.80	0.24	0.79	0.46	5.17	0.47	0.95	0.19
Illite																
WP+LL	0.55	0.20	0.59	0.73	7.16	6.76	3.52	2.73	1.75	1.07	1.34	1.33	0.80	0.85	0.55	0.54
UpperLzL	1.24	0.19	1.16	1.06	4.57	1.83	2.55	2.02	2.34	0.59	1.69	1.23	0.66	0.37	0.38	0.35
LowerLzL	1.50	0.19	1.47	1.29	7.19	5.30	3.64	4.70	3.32	1.55	2.56	3.42	1.01	1.11	0.71	1.39
MFd	0.11	0.04	0.09	1.20	4.21	3.18	2.80	3.65	1.43	0.26	1.05	1.52	0.78	0.41	0.76	0.99
UpperMFc	0.08	0.04	0.09	1.20	16.38	14.08	11.93	6.59	5.48	4.43	5.28	5.10	3.24	3.22	4.18	2.03
LowerMFc	0.03	0.05	0.04	0.71	11.78	17.94	2.79	0.91	0.80	0.99	1.07	1.01	1.66	1.98	1.01	0.14
Sudoite																
WP+LL	0.01	0.01	0.01	0.00	0.73	3.21	1.15	0.12	0.01	0.39	0.06	0.00	0.00	0.52	0.00	0
UpperLzL	0.01	1.03	0.01	0.00	0.16	4.30	0.03	0.00	0.01	1.89	0.01	0.00	0.00	0.49	0.00	0
LowerLzL	0.01	0.32	0.01	0.00	0.66	5.86	0.16	0.00	0.02	2.32	0.01	0.00	0.08	1.40	0.00	0
MFd	0.01	0.02	0.01	0.00	1.21	3.02	0.88	0.07	0.20	1.49	0.12	0.02	0.31	0.49	0.24	0.03
UpperMFc	0.01	0.01	0.01	0.00	4.92	12.46	0.52	0.06	0.28	1.16	0.03	0.01	0.74	1.68	0.11	0.02
LowerMFc	0.01	0.01	0.01	0.11	24.10	45.51	1.82	0.12	1.55	2.83	0.26	0.12	3.04	4.43	0.46	0.01
Dravite																
WP+LL	0.03	0.01	0.02	0.02	1.79	0.70	0.30	0.08	0.15	0.21	0.07	0.04	0.15	0.10	0.05	0.02
UpperLzL	0.03	0.07	0.03	0.03	0.95	0.70	0.13	0.05	0.12	0.23	0.06	0.03	0.14	0.13	0.03	0.01
LowerLzL	0.03	0.06	0.03	0.03	1.36	0.94	0.16	0.07	0.14	0.17	0.09	0.05	0.15	0.12	0.03	0.02
MFd	0.05	0.06	0.04	0.05	1.36	0.68	0.33	0.09	0.20	0.17	0.13	0.06	0.19	0.09	0.07	0.01
UpperMFc	0.04	0.03	0.06	0.06	4.17	2.12	0.84	0.13	0.34	0.24	0.19	0.08	0.51	0.24	0.15	0.02
LowerMFc	0.03	0.01	0.07	0.09	25.58	11.70	0.84	0.24	1.33	0.37	0.25	0.16	2.56	1.24	0.23	0.1

Hematite															
WP+LL	0.01	0.02	0.02	0.03	0.15	0.21	0.62	0.17	0.03	0.04	0.09	0.07	0.01	0.02	0.08	0.04
UpperLzL	0.01	0.02	0.03	0.04	0.04	0.08	0.12	0.14	0.03	0.04	0.06	0.07	0.01	0.01	0.02	0.03
LowerLzL	0.01	0.02	0.03	0.04	0.05	0.15	0.10	0.08	0.03	0.05	0.06	0.06	0.01	0.03	0.02	0.02
MFd	0.02	0.02	0.02	0.04	0.18	0.14	0.26	0.11	0.04	0.03	0.05	0.07	0.02	0.01	0.04	0.03
UpperMFc	0.01	0.02	0.02	0.06	0.20	0.20	0.26	0.20	0.04	0.04	0.07	0.12	0.02	0.02	0.06	0.05
LowerMFc	0.01	0.02	0.02	0.15		0.65	1.25	0.32	0.24		0.08	0.08	0.07	0.19		0.01
	0.09	0.06														
0.18																

Notes: The number of samples analyzed in the lower MFc, upper MFc, MFd, lower LzL, upper LzL and WP+LL formations, respectively: (a) Anne zone: 307, 137, 150, 127, 113, 45; (b) Colette zone: 285, 208, 123, 161, 131, 520; (c) distal drill holes: 14, 23, 41, 18, 22, 77; (d) drill hole Erica 1: 3, 6, 6, 4, 6, 21. Formation abbreviations: MF: Manitou Falls; LzL: Lazenby Lake; WP: Wolverine Point; LL: Locker Lake.

ment of kaolin with the kaolin being replaced by variable amounts of sudoite intergrown with illite, and not by illite alone (Laverret *et al.*, 2006, this issue). For most samples, the K values show a linear relationship with the Al contents, with the best-fit regression line having a slope of ~0.30. However, the sudoite-bearing samples display distinctly smaller K/Al ratios. If sudoite-bearing samples are excluded, the K/Al ratios are greater in the Anne area (and to a lesser extent also in the Colette area) compared to drill hole Erica 1, especially for the samples richest in Al (Figure 5). This feature indicates that the samples from the alteration halo have greater illite proportions than the background samples.

Normative kaolinite

The distribution of normative kaolinite is heterogeneous and does not continuously parallel the stratigraphy (Figure 6), unlike the Al_2O_3 distribution. Normative kaolinite is abundant in most of the formations present in the background drill hole Erica 1 (Figure 6a), in contrast to the other distal drill holes and particularly in contrast to the Anne and Colette mineralized areas (Figure 6b). For instance, the average kaolinite content is only 0.41 wt.% and 0.52 wt.% in the upper MFc Formation in the Anne and Colette areas, respectively, compared to 2.85 wt.% in drill hole Erica 1 (Table 2). The most kaolinite-depleted zones are located around the U ore bodies, in agreement with petrographic observations which revealed that the amount of kaolin decreases towards the Anne U ore body (Laverret *et al.*, 2006, this issue) due to replacement by illite and sudoite during host-rock alterations.

Normative sudoite

The configuration of the normative sudoite halo differs significantly from that of illite, as the presence of sudoite is limited to the mineralized areas (Figure 7). Sudoite occurs near the unconformity in both ore bodies, but not regionally. In the Colette area, the sudoite halo forms a large ‘plume’ that rises into the sandstone crosscutting the stratigraphy. High sudoite contents are observed up to 500 m above the unconformity (Figure 7b), in particular in the NW half of the section in the LzL and MFc Formations, where the illite contents are least (average contents of 2.32 wt.% and 2.83 wt.%, respectively, Table 2). In the Anne area, the sudoite halo is restricted to the lower MFc and locally to the MFd Formations.

Normative dravite

As with sudoite, normative dravite essentially only occurs in the mineralized zones. Above both the Anne and Colette ore bodies, dravite anomalies form ‘plumes’ that rise into the sandstone crosscutting the stratigraphy, but the dravite haloes rise higher into the sandstone than the sudoite haloes. In the Anne area, the narrow

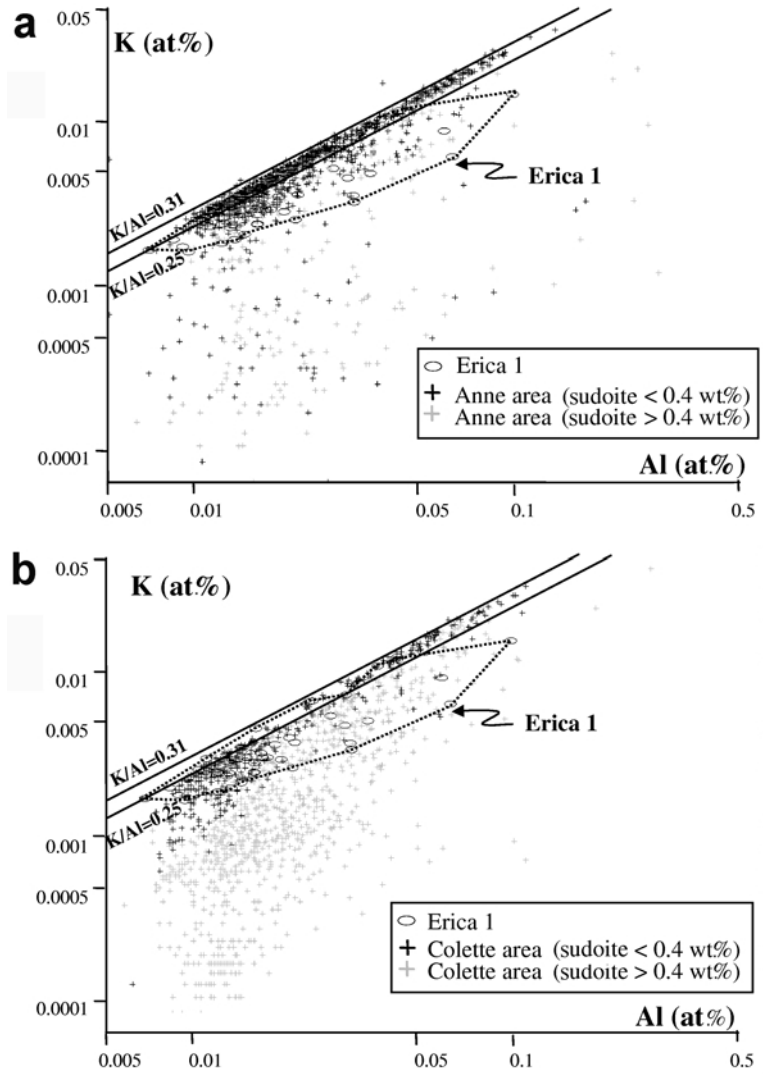

Figure 5. 2D scatterplot of K *vs*. Al (at.%). (a) Comparison between samples from drill hole Erica 1 and samples from the Anne area; (b) comparison between samples from drill hole Erica 1 and samples from the Colette area.

subvertical shape of the dravite anomaly up to 600 m above the unconformity suggests the presence of a fault/fracture network along which dravite developed. This is consistent with the petrographic features observed in samples representing the perched dravite anomalies, which reveal the presence of local tectonic breccias composed of quartz fragments cemented by microcrystalline quartz and dravite. In the Colette area, the extent of the dravite halo is larger and it rises 700 m up to the sandstone subcrop.

Normative hematite

The distribution of normative hematite in the distal section (Figure 6a) contrasts sharply with the hematite distribution in the mineralized areas (Figure 6b). Hematite is most abundant in the distal section, where it tends to be distributed in conformity with the stratigraphy. The largest hematite contents are found in the WP Formation and the basal MFc Formation (Table 2). This distribution is consistent with the distribution of the detrital heavy mineral beds containing hematite, after oxidation of titanomagnetite and ilmenite (Hoeve and Quirt, 1984), which are more abundant in coarser-grained intervals in the WP and MFc Formations (Collier *et al.*, 2001). Conversely, smaller hematite contents are observed above the SLC, predominantly in the Anne area (Figure 6b), due to the intensity of hematite dissolution (sandstone bleaching) during the host-rock alteration event(s), which is typically most intense near the mineralized areas (Hoeve and Quirt, 1984).

DISCUSSION

The diagenetic-hydrothermal model proposed for the genesis of sandstone-hosted unconformity-type U depos-

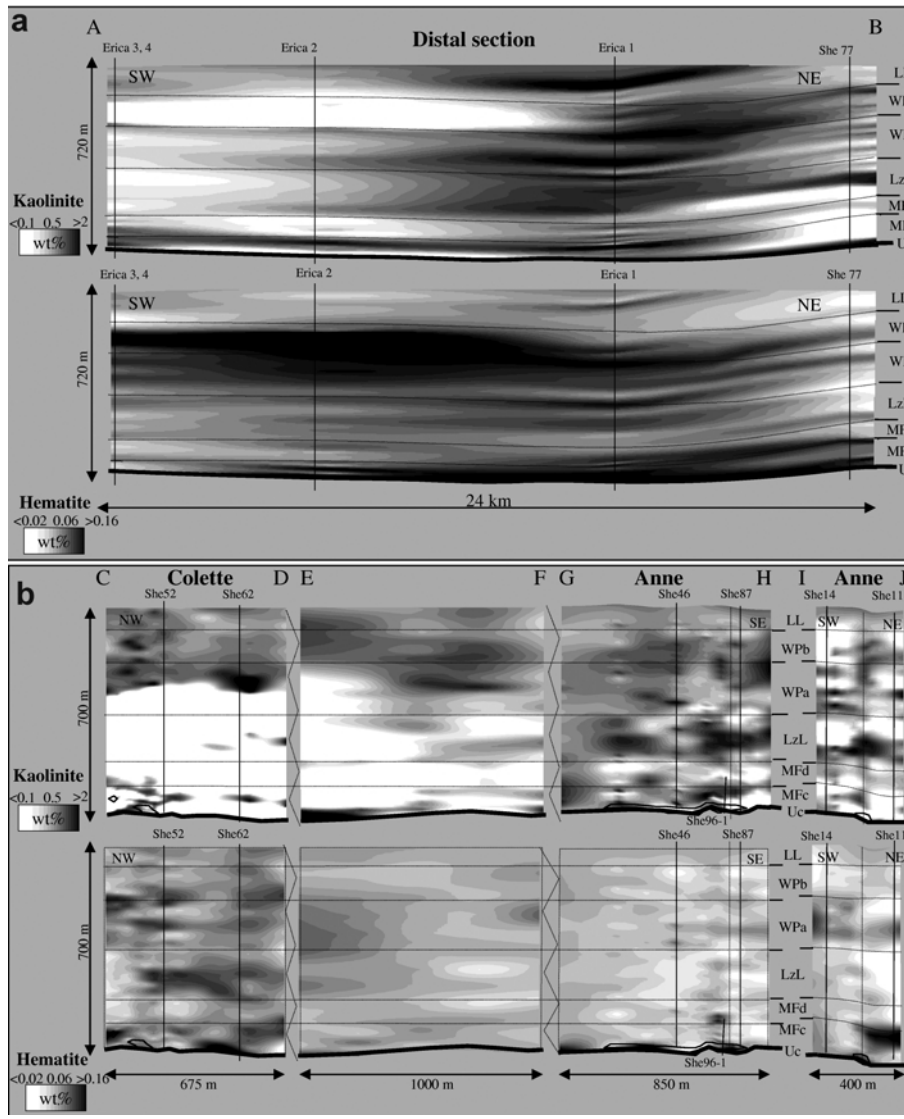

Figure 6. Kaolinite (upper) and hematite (lower) spatial distributions. The figure shows a vertical section across the 3D models (see Figure 1c). (a) Distal section, A–B, perpendicular to the SLC and constrained by five drill holes. Only drill hole Erica 1 did not intersect any basement-rooted structure. (b) Sections across the mineralized areas of Anne and Colette along the SLC (longitudinal sections: C–D, E–F, G–H; lateral section: I–J). See the caption of Figure 4 for comments and abbreviations.

its in the Athabasca Basin involves mixing of two brines, one from the Athabasca Group sandstone ('diagenetic' basinal brine), and one emerging from the basement along faults crosscutting the sub-Athabasca unconformity ('hydrothermal' basement-derived fluid; Hoeve and Sibbald, 1978; Hoeve and Quirt, 1984; Kotzer and Kyser, 1995). The present-day distributions of Athabasca Group matrix minerals around the U deposits result from the initial distribution of the detrital phases and then from the interactions between these two brines which mobilized the main cations (Al, K, Mg, B, Fe) constituting the alteration minerals. The mineral distributions presented in this study were compared to the lithostratigraphy and structural features (unconformity, presence of basement-rooted faults) of the Athabasca Group sandstone to determine the extent of the mobility of these elements during the diagenetic-hydrothermal event(s). Two element mobility-related processes can be distinguished: (1) a mass-transfer process involving element transfer from one mineral phase to another without displacement; and (2) a mass transport process involving element transport from an external source to the site of mineral alteration (Hutcheon, 2000).

Transfer of Al

The distribution of Al is conformable with the lithostratigraphy throughout the studied area, regardless of proximity to basement-rooted structures (Figure 4).

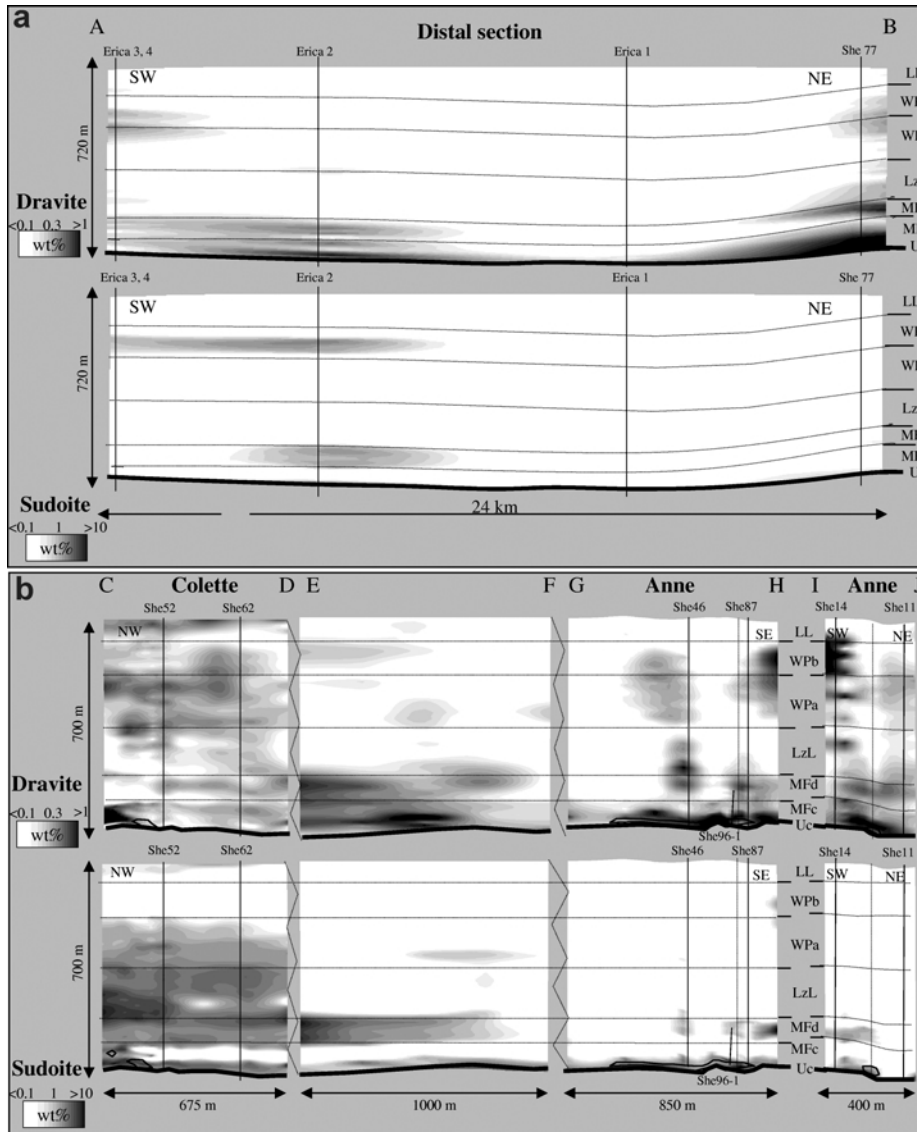

Figure 7. Dravite (top) and sudoite (bottom) spatial distributions. The figure shows a vertical section across the 3D models (see Figure 1c). (a) Distal section, A–B, perpendicular to the SLC and constrained by five drill holes. Only drill hole Erica 1 did not intersect any basement-rooted structure. (b) Sections across the mineralized areas of Anne and Colette along the SLC (longitudinal sections: C–D, E–F, G–H; lateral section: I–J). See the caption for Figure 4 for comments and abbreviations.

The only exceptions are the Al-rich host-rock alteration zones located immediately above the Anne and Colette ore bodies (Table 2). However, based on petrographic criteria and mass-balance calculations, these large Al contents correspond to dissolution breccia zones and consequently express relative clay enrichments due to volume loss caused by intense quartz dissolution (Lorilleux *et al*., 2002; 2003). If these breccia zones are excluded, the Al contents generally vary only with respect to the lithological units. The two units richest in Al are the upper MFc and lower LzL Formations which contrast strongly with the intervening Al-poor MFd Formation (Table 2). The stratigraphy-parallel distribution of Al may reflect either the initial deposition of Al-bearing detrital minerals or the formation-dependent, permeability-related transport of Al over large distances during diagenesis.

Large-scale mass transport of Al during diagenesis of clastic basins has been reported, such as in the sandstone reservoirs of the North Sea Central Graben (Wilkinson and Haszeldine, 1996, 1997). Based on mass-balance calculations, these authors proposed that a significant amount of Al was exported from the sandstone reservoirs to account for the small abundance of clay minerals despite a significant amount of feldspar dissolution. However, in their study, the mechanism of Al transport remained unexplained. Aluminum is commonly considered to be an immobile element because of its typically

low solubility at low temperatures (Drever, 1988; Salvi *et al*., 1998). In sandstone oil reservoirs, it has been suggested that the Al solubility may be increased due to the presence of organometallic ligands (Drummond and Palmer, 1986; Fein *et al*., 1994; Berger *et al*., 1997), but the presence of such organic ligands is very unlikely in the mid-Proterozoic intracontinental Athabasca Basin because no organic matter was present in the detritus.

The alternative interpretation that the present-day distribution of Al reflects the initial deposition of detrital Al-bearing minerals is supported by the lithofacies analysis of Collier (2002) based on the identification of primary sedimentary structures in the Shea Creek area. The upper MFc and lower LzL Formations are characterized by a relatively large proportion of clay mineral-rich silty units, compared to the MFd Formation, reflecting relatively humid fluvial depositional conditions favorable for the preservation of clay mineral-rich Al-bearing sediments. Conversely, the sedimentary structures in the MFd Formation are typical of relatively arid ephemeral river systems, in which such clay mineral-rich sediments would have been removed by eolian activity. Today, few Al-bearing detrital minerals are still preserved (rare white mica) and much of the detrital kaolinite has been recrystallized (kaolinite to dickite series) and then partly replaced by illite (Quirt, 2001; Laverret *et al*., 2006, this issue), as observed in other clastic sedimentary basins (Hurst and Irwin, 1982; Hoeve and Quirt, 1984; Lanson *et al*., 2002; Hiatt and Kyser, 2000; Hutcheon, 2000). In this context, Al was not transported, but was transferred from one mineral phase to another without significant movement. Before illitization, kaolin was therefore probably the dominant Al-bearing mineral.

Large-scale transport of K

The Shea Creek prospect is located within an extended (>50 km) 'regional illite anomaly' (Rippert *et al*., 2000). In this "regional illite anomaly" the conversion of kaolin to illite is more pronounced, even in the regional background samples from drill hole Erica 1, compared to other parts of the basin far from any known mineralization, as, for example, the Rumple Lake drill hole located near the middle of the Athabasca Basin (Hoeve and Quirt, 1984; Quirt, 2001). A similar regional illite anomaly is also present in the Eastern part of the Athabasca Basin, extending from the Key Lake deposit to the McArthur River deposit (Thomas *et al.*, 2000).

The illitization of kaolin depends on the availability of K, which may be present in detrital minerals (*e.g.* K-feldspar, K-mica) or which may be imported from an external source (Berger *et al*., 1997, 1999; Hutcheon, 2000; Lanson *et al*., 2002). In the former case K is transferred, whereas in the latter case, K must be transported to the site of mineral alteration.

In the Shea Creek region, the distribution of illite is conformable to the lithostratigraphy over the entire studied area (Figure 4), as typically observed in the Athabasca Group sandstone (Hoeve and Quirt, 1984; Quirt, 2001), suggesting that a potential source of K may have been inherited detrital K-bearing minerals (K-feldspar, K-mica), the distribution of which initially depended on the sedimentology. However, no preserved feldspar mineral grains have been observed in the Athabasca Group sandstones, and there is little petrographic evidence that they existed prior to diagenesis (Hoeve and Quirt, 1984; Ramaekers, 1990; Quirt, 2001; Laverret *et al*., 2006, this issue). Detrital micas are present in the Athabasca Group, but in very small amounts, and petrographic observations show that they have been well preserved, with no evidence of illitization, suggesting that detrital mica was not a source of K to the system. Therefore detrital K-feldspars and K-micas probably did not constitute a sufficient reservoir of K to explain the Shea Creek regional illite anomaly.

The other possible source of K is the sub-Athabasca basement because it contains highly potassic plutonites and K-rich metasediments (Table 3), especially in the Shea Creek area (Pagel and Svab, 1985; Card, 2002; Brouand and Cuney, 2002). These rocks are typically intensely altered along the faults intersecting the unconformity (Hoeve and Quirt, 1984; Pagel and Svab, 1985), with almost total dissolution of K-feldspar and crystallization of illite (Laverret *et al.*, 2006, this issue). Illites present along these structures display similar crystal-chemical characteristics both above and below the unconformity (Laverret *et al.*, 2006, this issue), suggesting that the faulted basement rocks were permeable to basinal fluids and that K released from altered basement K-feldspar was probably transported to the sandstone via fault zones. This model is consistent with the overall more pronounced conversion of kaolin observed in zones proximal to the basement-rooted structures (Anne and Colette areas, Figure 6b) where the greatest K^+/H^+ ratios were probably attained (Hoeve and Quirt, 1984; Raffensperger and Garven, 1995). Conversely, background samples from drill hole Erica 1 display greater kaolin proportions (Figure 6, Table 2) and lower K/Al ratios (if the sudoite-bearing samples are excluded; Figure 5).

Assuming that this K was essentially supplied to the sandstone cover by the alteration of basement K-feldspar and mica through transport via fault zones crosscutting the sub-Athabasca unconformity, the variable but continuous occurrence of illite in the Shea Creek regional illite anomaly, including drill hole Erica 1 (Figure 4), then implies that K has been transported laterally at least several kilometers from the basement-rooted faults. As Al was probably relatively immobile (see above), the distribution of illite in conformity with the lithostratigraphy and the positive correlation between K and Al for sudoite-free samples (Figure 5) suggests that the amount of K present in the sandstone was controlled by the

Table 3. Estimated amounts of basement rocks to be leached to account for the K and Mg enrichments observed in the Anne and Colette alteration haloes, considering the major basement rock types occurring in this part of the Athabasca Basin.

Basement rock types		K_2O (wt.%)	MgO (wt.%)	Amount (tonnes) of basement rock containing: 1.86×10^5 t K[(c)]	6.61×10^4 t Mg[(c)]	2.42×10^4 t K[(d)]	1.85×10^5 t Mg[(d)]
Metasediments	Aluminous gneiss	[(a)] 3.96	2.49	5.67×10^6	4.40×10^6 [(e)]	7.39×10^5	1.23×10^7
		[(b)] 2.97	2.5	7.55×10^6	4.38×10^6 [(e)]	9.85×10^5	1.23×10^7
	Feldspathic gneiss	[(a)] 5.35	2.04	4.19×10^6	5.36×10^6 [(e)]	5.47×10^5	1.50×10^7
		[(b)] 7.26	1.66	3.09×10^6	6.59×10^6 [(e)]	4.03×10^5	1.85×10^7
Plutonic rocks	Granitoids/pegmatoids	[(a)] 4.45	0.38	5.04×10^6	2.88×10^7	6.57×10^5	8.06×10^7
		[(b)] 6.32	0.58	3.55×10^6	1.89×10^7	4.65×10^5	5.28×10^7
Restites	Mafic gneiss	[(a)] 2.7	15.2	8.31×10^6	7.20×10^5	1.08×10^6	2.02×10^6 [(f)]
		[(b)] 1.52	8.25	1.48×10^7	1.33×10^6	1.92×10^6	3.71×10^6 [(f)]

Notes: (a) average K_2O and MgO contents from Pagel and Svab (1985); (b) average K_2O and MgO contents in the Anne mineralized area (M. Brouand, unpublished data, 1998); (c) excess amount in the Anne alteration halo (Table 1); (d) excess amount in the Colette alteration halo (Table 1); (e) the values obtained for K with these rock types are similar to those obtained for Mg, suggesting that leaching of these rock types may provide the necessary amounts of both K and Mg in the Anne alteration halo, keeping the observed K/Mg ratio, while for the plutonic rocks and restites, the calculated values for K and Mg differ by more than one order of magnitude, thus requiring the alteration of a second type of rock; (f) as for (e), except that leaching of mafic gneiss best accounts for the lower K/Mg ratio observed in the Colette alteration halo.

initial quantity of Al-bearing minerals (*i.e.* kaolin). The homogeneous chemical compositions obtained for illites in the mineralized areas and in the distal drill holes (Laverret *et al.*, 2006, this issue), and the $^{87}Sr/^{86}Sr$ radiogenic isotope data and stable isotope data of illites from different locations in the eastern part of the Athabasca Basin (Armstrong and Ramaekers, 1985; Percival *et al.*, 1993; Kotzer and Kyser, 1995) support the possibility of extensive lateral movements of the fluid involved in the illitization process.

Structure-controlled transport of Mg and B

The configurations of the dravite and sudoite haloes that rise from the unconformity to upper sandstone formations cross-cutting the stratigraphy (Figure 7) suggest that Mg and B were transported from the basement to the sandstone cover via fault zones. This interpretation is supported by the absence of Mg-bearing detrital minerals in unaltered sandstone, with only biotite as rare solid inclusions in detrital quartz being observed, whereas, in the basement, abundant altered mafic minerals (*e.g.* garnet, biotite, cordierite) are found around the fault zones (Hoeve and Quirt, 1984; Pagel and Svab, 1985). Although very minor amounts of authigenic dravite are present as overgrowths on detrital Fe-tourmaline in the Athabasca Group sandstone (Quirt *et al.*, 1991; Pacquet and Weber, 1993), the source of B for the dravite in the alteration haloes was probably the basement because of its larger average B contents (~40 ppm, Pagel and Svab, 1985) relative to unaltered sandstone (~19 ppm in background sandstone). Sudoite and dravite formation was restricted to the vicinity of the fault zones, confirming that it is in these zones that the Mg and B activities of the fluid emerging from the basement were the greatest (Hoeve and Quirt, 1984; Raffensperger and Garven, 1995).

The location of the dravite and sudoite anomalies over the mineralized areas (Figure 7b) suggests that formation of these minerals was contemporaneous with the mineralizing event(s). This is confirmed by petrographic observations of samples around the Anne ore body (Laverret *et al.*, 2006, this issue), which show sudoite to be finely intergrown with illite and both intimately associated with dravite needles.

Structure-controlled hematite removal

The small hematite contents and the intense hematite removal (sandstone bleaching) features observed above the Anne and Colette mineralized areas, in particular within the sudoite and dravite anomalies (Figure 6, Table 2), suggest that hematite dissolution occurred during the host-rock alteration event(s). Dissolved Fe may have been lost from the sandstone (Fe transport) and/or incorporated in the alteration minerals composed of sudoite, dravite, and/or illite (Fe transfer), although these minerals contain little Fe. Hematite bleaching probably resulted from the circulation of reducing fluids,

as the Athabasca Basin paleobrines were chloride-rich brines (Derome *et al*., 2003) and in such fluids Fe is typically transported as Fe(II) chloride complexes ($FeCl_2$ or $FeCl^+$; Heinrich and Seward, 1990). Such reducing conditions would have been promoted by the destabilization of Fe^{2+}-bearing minerals and/or graphite in the basement (Hoeve and Sibbald, 1978; Hoeve and Quirt, 1984; Raffensperger and Garven, 1995; Komninou and Sverjensky, 1996). The 'bleaching' halo (Figure 6) consequently records the advancement of a reducing front from the basement towards and into initially oxidized, hematite-bearing sandstone.

Mass-balance considerations

Relative to the samples from drill hole Erica 1 for the background B and Mg contents of unaltered Athabasca Group sandstone in the Shea Creek area, the sudoite and dravite haloes above the U ore bodies (Figure 7) represent a calculated excess amount of ~66,000 t of Mg and 11,000 t of B in the Anne area, and up to 185,000 t of Mg with a similar amount of B in the Colette area (Table 1). Mass-balance calculations for K are more difficult to interpret because the illite haloes extend beyond the modeled areas and K possibly migrated as far as drill hole Erica 1. Even so, the illite haloes in the Anne and Colette areas would represent enrichments of ~186,000 t and 24,000 t of K, respectively (Table 1).

These considerations highlight major differences in the distribution and geochemistry of the alteration haloes between the two ore zones. Compared to the Colette area, the Anne alteration halo is characterized by (1) a less-extensive sudoite-dravite halo (~0.04 km^3 *vs.* ~0.08 km^3, Table 1) which is restricted to the fault zones (Figure 7), and (2) a significant K enrichment relative to Mg (average K/Mg ratio of 2.8 *vs*. 0.13, Table 1).

The first difference is due to the presence of a pre-host-rock alteration silica cap over the Anne U ore body (Lorilleux *et al*., 2002) which is not present in the Colette area. This silicified zone may have acted as an impermeable barrier which restricted the basement fluid infiltration to permeable structures. Conversely, in the Colette area which lacks such a silicified zone, the fluids would have dispersed more widely in the rock porosity. Similar observations have been made at the McArthur River deposit (McGill *et al*., 1993) which has a pre-ore silica cap present up to 150 m above the unconformity and a spatially-restricted clay mineral alteration halo despite its very high grade and tonnage.

The difference between the K/Al ratios may result from variations in basement rock composition, assuming that basement rocks constitute the main source of K and Mg. A relationship between the mineralogical and chemical characters of the host-rock alteration and the composition of the leached underlying basement rocks has been demonstrated for other deposits of the Athabasca Basin: illite dominates the host-rock alteration halo where the basement consists of K-rich quartzo-feldspathic rocks (*e.g.* Midwest, McClean and Key lake deposits), while chlorite dominates where the basement consists of Mg-rich marbles and calc-silicate gneisses (e.g. Rabbit Lake and Dawn Lake deposits; Hoeve and Quirt, 1984; Thomas *et al*., 2000). In the Shea Creek region, basement rocks include plutonic rocks, metasediments and minor restites, with variable K/Mg ratios (Table 3). To balance the excess amounts of K and Mg contained in the Anne alteration halo, it is estimated that leaching of approximately 5×10^6 t of metasedimentary rocks would be needed (Table 3). In the Colette alteration halo, the stronger Mg enrichment relative to K may be better accounted for by leaching of approximately 2×10^6 t of mafic gneiss, which have smaller K/Mg ratios compared to metasediments (Table 3). However, such variations in basement rock compositions remain to be demonstrated between these two ore zones, which are only 1.5 km apart along the same structure.

CONCLUSIONS

Two complementary approaches were combined to quantitatively represent the spatial distribution of the Athabasca Group sandstone matrix minerals at a regional scale (~25 km): (1) detailed petrographic and XRD studies on specific representative samples, and (2) normative mineral calculations and 3D interpolation using a large number of samples of known major element compositions and spatial locations. Knowing that similar mineral assemblages, although with variable proportions (Hoeve and Quirt, 1984; Kotzer and Kyser, 1995; Thomas *et al*., 2000), are observed in other Athabasca U deposits, those 3D models may be extended to other locations in the Athabasca Basin, where sufficient geochemical data are available.

The results of this study confirm the current diagenetic-hydrothermal model proposed for the genesis of sandstone-hosted unconformity-type U deposits in the Athabasca Basin (Hoeve and Sibbald, 1978; Hoeve and Quirt, 1984; Kotzer and Kyser, 1995). They illustrate the advancement of a fluid emerging from the basement upward toward the sandstone *via* basement-rooted faults, along which U was also precipitated. In addition, quantitative data are provided to constrain the origin of authigenic minerals in the sandstone, and the operation of mass transport processes *vs.* mass transfer processes (*in situ* redistribution of elements). It has been determined that (1) neoformation of illite, sudoite and dravite in the Athabasca Group sandstone required the transport of K, Mg and B from an external source (~10^4–10^5 t above the Anne and Colette ore bodies), (2) various amounts of these elements may be transported depending on the mineralogy of the underlying basement lithologies, and (3) in contrast to B and Mg, K may be

transported laterally at least several km from the basement-rooted faults.

ACKNOWLEDGMENTS

The authors thank COGEMA, Cogema Resources Incorporated and Cluff Lake Mine geologists for their financial and technical support. We gratefully acknowledge J.-J. Royer and C. Le Carlier de Veslud (ENSG, Nancy, France) for their contribution to the GOCAD modeling, and W.C. Elliott and J.B. Percival for their critical reviews and constructive comments.

REFERENCES

Armstrong, R.L. and Ramaekers, P. (1985) Sr isotopic study of Helikian sediment and basaltic dykes in the Athabasca Basin, northern Saskatchewan. *Canadian Journal of Earth Sciences*, **22**, 399–407.

Beaufort, D., Cassagnabère, A., Petit, S., Lanson, B., Berger, G., Lacharpagne, J.-C. and Johansen, H. (1998) Kaolinite-to-dickite reaction in sandstone reservoir. *Clay Minerals*, **33**, 297–316.

Berger, G., Lacharpagne, J.-C., Velde, B., Beaufort, D. and Lanson, B. (1997) Kinetic constraints on illitization reactions and the effect of organic diagenesis in sandstone/shales sequences. *Applied Geochemistry*, **12**, 23–35.

Berger, G., Velde, B. and Aigouy, T. (1999) Potassium sources and illitization in Texas Gulf Coast shale diagenesis. *Journal of Sedimentary Research*, **69**, 151–157.

Billaut, V., Beaufort, D., Patrier, P. and Petit, S. (2002) Crystal chemistry of Fe-sudoites from uranium deposits in the Athabasca Basin (Saskatchewan, Canada). *Clays and Clay Minerals*, **50**, 70–81.

Brouand, M. and Cuney, M. (2002) Age and nature of the plutonism of the western part of the Athabasca basin basement (northern Saskatchewan, Canada). *GAC-MAC Joint Annual Meeting*, Saskatoon, SK, Abstracts volume **27**, p. 14.

Card, C.D. (2002) New investigations of basement to the western Athabasca Basin. Pp. 1–17 in: *Summary of Investigations 2002*, Volume **2**, Saskatchewan Geological Survey, Miscellaneous Report 2002-4.2.

Collier, B. (2002) Detailed stratigraphy and facies analysis of the Paleoproterozoic Athabasca Group along the Shea-Creek-Douglas River transect, northern Saskatchewan. Pp. 1–16 in: *Summary of Investigations 2002*, Volume **2**, Saskatchewan Geological Survey, Miscellaneous Report 2002-4.2.

Collier, B., Yeo, G., Long, D., Robbins, J. and Koning, E. (2001) Preliminary report on the stratigraphy of the Athabasca Group in the vicinity of the Shea Creek project, southwestern Athabasca Basin. Pp. 266–271 in: *Summary of Investigations 2001*, Volume **2**, Saskatchewan Geological Survey, Miscellaneous Report 2001-4.2.

Derome, D., Cathelineau, M., Cuney, M. and Fabre, C. (2003) Reconstitution of the P, T, X characteristics of paleofluids in the McArthur River unconformity-type uranium deposit (Saskatchewan, Canada). Pp. 141–144 in: *Uranium Geochemistry 2003* (M. Cuney, editor). International Conference Proceedings, UMR-CNRS 7566 G2R, Nancy, France.

Drever, J.I. (1988) Stability relationships and silicate equilibria. Pp. 99–123 in: *The Geochemistry of Natural Waters* (J. I. Drever, editor). Prentice Hall, New Jersey.

Drummond, S.A. and Palmer, D.A. (1986) Thermal decarboxylation of acetate. Part II. Boundary conditions for the role of acetate in the primary migration of natural gas and the transportation of metals in hydrothermal systems. *Geochimica et Cosmochimica Acta*, **50**, 825–833.

Fein, J.B., Yane, L. and Handa, T. (1994) The effect of aqueous complexation on the decarboxylation rate of oxalate. *Geochimica et Cosmochimica Acta*, **58**, 3975–3981.

Garven, G. and Raffensperger, J.P. (1997) Hydrogeology and geochemistry of ore genesis in sedimentary basins. Pp. 125–189 in: *Geochemistry of Hydrothermal Ore Deposits* (H.L. Barnes, editor). John Wiley & Sons, New York.

Heinrich, C.A. and Seward, T.M. (1990) A spectrophotometric study of aqueous iron (II) chloride complexation from 25ºC to 200ºC. *Geochimica et Cosmochimica Acta*, **54**, 2207–2221.

Hiatt, E. and Kyser, K. (2000) Links between depositional and diagenetic processes in basin analysis: an overview of porosity and permeability evolution in sedimentary rocks. Pp. 63–90 in: *Fluids and Basin Evolution* (K. Kyser, editor). Short Course Series **28**, Mineralogical Association of Canada.

Hoeve, J. and Quirt, D. (1984) *Mineralization and host rock alteration in relation to clay mineral diagenesis and evolution of the middle-Proterozoic Athabasca Basin, northern Saskatchewan, Canada*. SRC Technical Report 187, Saskatchewan Research Council, 187 pp.

Hoeve, J. and Sibbald, T.I.I. (1978) On the genesis of Rabbit Lake and other unconformity-type uranium deposits in northern Saskatchewan, Canada. *Economic Geology*, **73**, 1450–1473.

Hurst, A. and Irwin, H. (1982) Geological modeling of clay diagenesis in sandstones. *Clay Minerals*, **17**, 5–22.

Hutcheon, I. (2000) Principles of diagenesis and what drives mineral change. Pp. 93–114 in: *Fluids and Basin Evolution* (K. Kyser, editor). Short Course Series, **28**, Mineralogical Association of Canada.

Jambor, J.L. and Dilabio, R.N. (1978) *Distribution of hydrothermal clays in the Highland Valley copper porphyry deposit, British Columbia.* Geological Survey of Canada Paper 77-90.

Komninou, A. and Sverjensky, D.A. (1996) Geochemical modeling of the formation of an unconformity-type uranium deposit. *Economic Geology*, **91**, 590–606.

Kotzer, T.G. and Kyser, T.K. (1995) Petrogenesis of the Proterozoic Athabasca Basin, northern Saskatchewan, Canada, and its relation to diagenesis, hydrothermal uranium mineralization and paleohydrogeology. *Chemical Geology*, **120**, 45–89.

Kyser, K. and Hiatt, E.E. (2003) Fluids in sedimentary basins: an introduction. *Journal of Geochemical Exploration*, **80**, 139–149.

Lanson, B., Beaufort, D., Berger, G., Bauer, A., Cassagnabère, A. and Meunier, A. (2002) Authigenic kaolin and illitic minerals during burial diagenesis of sandstones: a review. *Clay Minerals*, **37**, 1–22.

Laverret, E. (2002) Les paragénèses argileuses associées aux gisements d'uranium sous discordance, secteur de Shea Creek (Bassin de l'Athabasca, Canada). PhD thesis, Université de Poitiers, France, 192 pp.

Laverret, E., Patrier Mas, P., Beaufort, D., Kister, P., Quirt, D., Bruneton, P. and Clauer, N. (2006) Mineralogy and geochemistry of the host-rock alterations associated with the Shea Creek unconformity-type uranium deposits (Athabasca Basin, Saskatchewan, Canada) Part 1. Spatial variation of illite properties. *Clays and Clay Minerals*, **54**, 275–294.

Lorilleux, G., Jébrak, M., Cuney, M. and Baudemont, D. (2002) Polyphase hydrothermal breccias associated with unconformity-type uranium mineralization (Canada): from fractal analysis to structural significance. *Journal of Structural Geology*, **24**, 323–338.

Lorilleux, G., Cuney, M., Jébrak, M., Rippert, J.C. and Portella, P. (2003) Chemical brecciation processes in the Sue unconformity-type uranium deposits, Eastern Athabasca Basin (Canada). *Journal of Geochemical Exploration*, **80**, 241–258.

Mallet, J.-L. (1992) Discrete smooth interpolation. *Computer Design*, **24**, 178–191.

McGill, B.D., Marlartt, J.L., Matthews, R.B., Sopuck, V.J. and Homeniuk, L.A. (1993) The P2 North Uranium Deposit, Saskatchewan, Canada. *Exploration and Mining Geology*, **2**, 321–331.

Pacquet, A. and Weber, F. (1993) Pétrographie et minéralogie des haloes d'altération autour du gisement de Cigar Lake et leurs relations avec les minéralisations. *Canadian Journal of Earth Science*, **30**, 674–688.

Pagel, M. and Svab, M. (1985) Petrographic and geochemical variations within the Carswell Structure metamorphic core and their implications with respect to uranium mineralization. Pp. 55–70 in: *The Carswell Structure Uranium Deposits, Saskatchewan*, (R. Lainé, D. Alonso and M. Svab, editors). Special paper **29,** Geological Association of Canada.

Percival, J.B., Bell, K. and Torrance, J.K. (1993) Clay mineralogy and isotope geochemistry of the alteration halo at the Cigar Lake uranium deposit. *Canadian Journal of Earth Sciences*, **30**, 689–704.

Quirt, D.H. (1995) *Norm calculation procedure for sandstone clay minerals*. Publicaton R-1230-28-E-95, Saskatchewan Research Council, Canada, 14 pp.

Quirt, D.H. (2001) *Kaolinite and dickite in the Athabasca Sandstone, northern Saskatchewan, Canada*. Publication 10400-16D01, Saskatchewan Research Council, Canada, 27pp.

Quirt, D., Kotzer, T. and Kyser, T.K. (1991) Tourmaline, phosphate minerals, zircon and pitchblende in the Athabasca Group: Maw Zone and McArthur River areas, Saskatchewan. Pp. 181–191 in: *Summary of Investigations 1991*, Saskatchewan Geological Survey, Miscellaneous Report 1991-4.

Raffensperger, J.P. and Garven, G. (1995) The formation of unconformity-type uranium ore deposits. 2. Coupled hydrochemical modeling. *American Journal of Science*, **295**, 639–696.

Ramaekers, P. (1990) *Geology of the Athabasca Group (Helikian) in Northern Saskatchewan*. Report 195, Saskatchewan Geological Survey, Canada, 49 pp.

Ramaekers, P., Yeo, G. and Jefferson, G. (2001) Preliminary overview of regional stratigraphy in the Late Paleoproterozoic Athabasca Basin, Saskachewan and Alberta. Pp. 240–251 in: *Summary of Investigations 2001*, Volume **2**, Saskatchewan Geological Survey, Miscellaneous Report 2001-4.2, Canada.

Reed, M.H. (1997) Hydrothermal alteration and its relationship to ore fluid composition. Pp. 303–366 in: *Geochemistry of Hydrothermal Ore Deposits* (H.L. Barnes, editor). John Wiley & Sons, Inc., New York.

Rippert, J.C., Koning, E., Robbins, J., Koch, R. and Baudemont, D. (2000) The Shea Creek Uranium Project, West Athabasca Basin, Saskatchewan, Canada. Abstract 570 in *Proceedings of Geo Canada 2000, The Millennium Geoscience Summit*. GAC-MAC joint annual meeting, Calagary.

Salvi, S., Pokrovski, G.S. and Schott, J. (1998) Experimental investigation of aluminium-silica aqueous complexing at 300ºC. *Chemical Geology*, **151**, 51–67.

Skinner, B.J. (1997) Hydrothermal mineral deposits: what we do and don't know. Pp. 1–29 in: *Geochemistry of Hydrothermal Ore Deposits* (H.L. Barnes, editor), John Wiley & Sons, Inc., New York.

Thomas, D.J., Matthews, R.B. and Sopuck, V. (2000) Athabasca Basin (Canada) Unconformity-Type Uranium Deposits: Exploration Model, Current Mine Developments and Exploration Directions. Pp. 1–23 in: *Geology and Ore Deposits 2000: The Great Basin and Beyond*, Geological Society of Nevada, USA.

Wilkinson, M. and Haszeldine, R.S. (1996) Aluminium loss during sandstone diagenesis. *Journal of the Geological Society, London*, **153**, 657–660.

Wilkinson, M. and Haszeldine, R.S. (1997) Discussion on aluminium loss during sandstone diagenesis. *Journal of the Geological Society, London*, **154**, 747–751.

Wilson, J.A. (1984) Crandallite group minerals in the Helikian Athabasca Group in Alberta, Canada. *Canadian Journal of Earth Sciences*, **22**, 637–641.

(*Received 31 May 2004; revised 2 May 2005; Ms. 921; A.E. W. Crawford Elliott*)